

# Synthesis of a Neo-Confused Octaphyrin and the Formation of Its Mononuclear Complexes

Kai Zhang,<sup>†</sup> Junda Zhang,<sup>†</sup> Xin Li,<sup>‡</sup> Rui Guo,<sup>§</sup> Hans Ågren,<sup>‡</sup> Zhongping Ou,<sup>§</sup> Masatoshi Ishida,<sup>||</sup> Hiroyuki Furuta,<sup>\*,||</sup> and Yongshu Xie<sup>\*,†</sup>

<sup>†</sup>Key Laboratory for Advanced Materials and Institute of Fine Chemicals, East China University of Science and Technology, Shanghai 200237, P. R. China

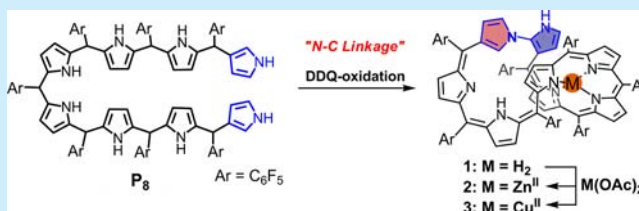
<sup>‡</sup>Department of Theoretical Chemistry and Biology, School of Biotechnology, KTH Royal Institute of Technology, Stockholm Se-10691, Sweden

<sup>§</sup>School of Chemistry & Chemical Engineering, Jiangsu University, Zhenjiang 212013, P. R. China

<sup>||</sup>Center for Molecular Systems, Department of Chemistry and Biochemistry, Graduate School of Engineering, Education Center for Global Leaders in Molecular Systems for Devices, Kyushu University, Fukuoka 819-0395, Japan

**S** Supporting Information

**ABSTRACT:** Novel neo-confused octaphyrin(1.1.1.1.1.1.0) (**1**) was synthesized by oxidative ring closure of an octapyrrole bearing two terminal “confused” pyrroles. Crystal structures of its Zn(II) and Cu(II) complexes (**2** and **3**) show a figure-of-eight conformation with unique mononuclear coordination structures. Photophysical data and theoretical calculations suggest that the neo-confused octaphyrin **1** is a 34 $\pi$  electron conjugated species showing nonaromaticity. Coordination of copper and zinc ions results in the further narrowing of the HOMO–LUMO gaps.



In recent years, porphyrin analogues have attracted great attention because of their rich structural diversities and interesting properties which are often different from those of regular porphyrins.<sup>1</sup> Contraction of the distinct  $\pi$ -framework of the tetrapyrroles gives, for example, corroles possessing a  $C_\alpha$ – $C_\alpha$  linked bipyrrrole unit, which alters the metal coordination abilities and their reactivities.<sup>2</sup> Increasing the number of pyrroles of the parent macrocycle, on the other hand, gives rise to expanded porphyrinoids, which demonstrate unique properties such as near-infrared absorption, facile redox reaction, and topological aromaticity.<sup>3</sup> In the past two decades, we have been working on the synthesis of porphyrin mutants containing “confused pyrrole ring” units linked through the  $\alpha,\beta'$  positions (known as N-confused porphyrins<sup>4–7</sup>) to open up new areas of  $\pi$ -material applications. In addition, Lash and co-workers recently developed neo-confused porphyrins with one of the confused pyrroles linked through its  $N,C_{\text{meso}}$  positions.<sup>1i,j</sup> Combining these design approaches, a series of N-confused-contracted as well as -expanded porphyrinoid have been reported (selected examples are shown in Figure 1).<sup>8–10</sup> In particular, oxidative ring closure reactions of linear oligopyrroles containing one or two terminal  $\beta$ -linked pyrroles afforded unprecedented cyclic products, such as N– $C_\alpha$  linked neo-confused corrole<sup>7b</sup> and hexaphyrin.<sup>10</sup> Interestingly, the directly linked confused pyrroles showed synergic high reactivities accompanied by unique macrocycle interconversion reactions under mild conditions.<sup>9,10</sup> It is noteworthy that a pyrrolic nitrogen atom plays an important role in the  $\pi$ -

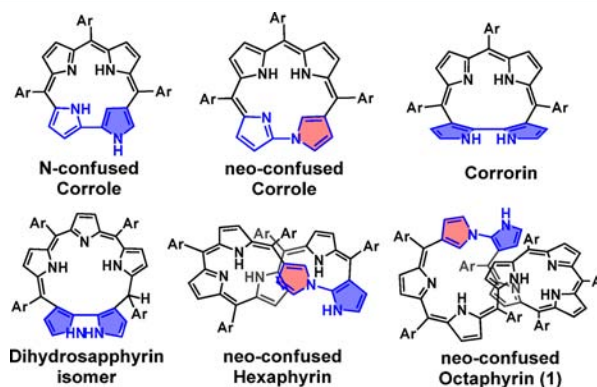


**Figure 1.** Structures of N-confused and N-linked porphyrinoids containing various bipyrrrole units.

conjugation through the  $C_\alpha$ –N bonding fashion. In this respect, the structural relationship between the connection modes (e.g., N– $C_\alpha$  vs  $C_\alpha$ – $C_\alpha$ ) and the number of  $\pi$ -electron conjugation components (e.g., tetra-, penta-, hexa-pyrrolic systems) have not yet been explored in detail. Research on the corresponding longer chain compounds is particularly desired.

In this study, we have synthesized a novel N-linked octaphyrin(1.1.1.1.1.1.0) (**1**) through an oxidative ring

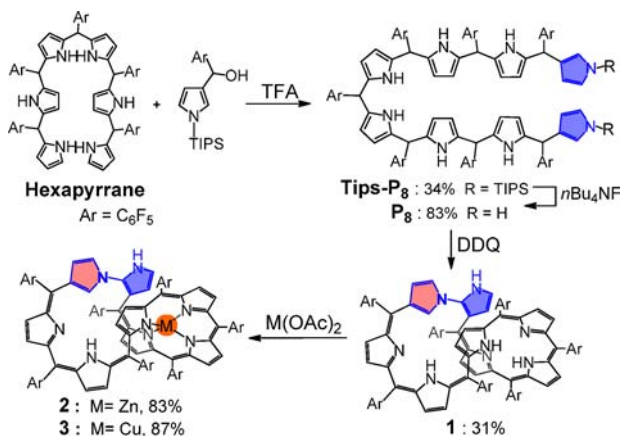
**Received:** August 16, 2015

**Published:** September 14, 2015

closure reaction of an octapyrrene derivative embedded with two terminal confused pyrroles ( $P_8$ ). Coordination of  $1$  with  $Zn^{II}$  and  $Cu^{II}$  ions afforded figure-of-eight shaped mononuclear complexes,  $2$  and  $3$ , respectively. The spectroscopic and theoretical studies suggested the distinct nonaromatic nature of the macrocycles.

Details of the syntheses are outlined in Scheme 1. The key precursor,  $P_8$ , was synthesized by acid-catalyzed condensation

**Scheme 1. Synthesis of Compounds 1–3 (Ar =  $C_6F_5$ )**



of the corresponding hexapyrrene<sup>11</sup> with *N*-triisopropylsilyl  $\beta$ -pyrrole carbinol, followed by deprotection with tetra-*n*-butylammonium fluoride.<sup>10</sup> Then, octapyrrene  $P_8$  was oxidized with 5.5 equiv of 2,3-dichloro-5,6-dicyano-1,4-benzoquinone (DDQ) to afford the neo-confused octapyrrenin  $1$  in a 31% yield.

The 400 Mz  $^1H$  NMR spectrum of  $1$  in  $CDCl_3$  exhibits 17 pyrrolic CH protons in the typical lower field region (Figure 2).

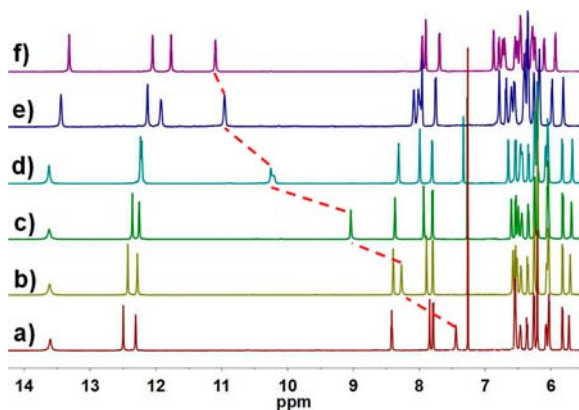


**Figure 2.** Low field region of 400 Mz  $^1H$  NMR spectra of  $1$  in different ratios of  $DMSO-d_6$  and  $CDCl_3$  at 298 K: (a) 0.5 mL  $CDCl_3$ ; (b–d) 0.5 mL  $CDCl_3$  +  $1$ , 3, or 20  $\mu L$   $DMSO-d_6$ ; (e) 0.25 mL  $CDCl_3$  + 0.25 mL  $DMSO-d_6$ ; (f) 0.5 mL  $DMSO-d_6$ .

Considering the original number of protons in  $P_8$ , disappearance of a CH proton is indicative of the macrocycle formation through generation of an interpyrrolic C–N bond between the CH and NH moieties, which is consistent with the neo-confused octapyrrenin structure as revealed by the crystal structures of  $2$  and  $3$  (vide infra). Accordingly, the mass spectrum of  $1$  showed the corresponding molecular ion peak of the proposed structure at  $m/z = 1770.288$ . It is noteworthy that the chemical shift of a specific NH resonance peak appeared at

$\delta = 7.44$  ppm (observed in  $CDCl_3$ ) and was found to be highly dependent on the solvent (Figures 2 and S12). Upon gradual addition of  $DMSO-d_6$ , the signal was significantly shifted to lower field, reaching 11.10 ppm in  $DMSO-d_6$  (i.e.,  $\Delta\delta = 3.66$  ppm) (Figure 2), whereas the other three NH peaks at  $\delta = 13.62$ , 12.49, and 12.30 ppm (in  $CDCl_3$ ), respectively, are insensitive to the solvents. This result indicates that this NH is involved in intermolecular hydrogen bonding with the solvent molecules, and thus it may be assigned as an outer NH. Furthermore, the NMR spectra in  $CDCl_3$  clearly exhibited one set of protons without obvious changes within  $-60$ – $20$  °C (Figure S13), and thus, the possibility of conformational changes could be ruled out. The overall NMR spectral features of  $1$  thus suggest that the macrocycle  $1$  shows no characteristic diatropic ring current (Figures 2 and S3).

To date, various octapyrrenin derivatives have demonstrated coordination ability with various transition metal ions as binucleating ligands.<sup>12</sup> Therefore, the octapyrrenin  $1$  was tested for coordination (Scheme 1). A solution of  $1$  in methanol was heated at reflux in the presence of 10 equiv of  $Zn(OAc)_2 \cdot 2H_2O$  for 2 h to afford complex  $2$  in a yield of 83%. The corresponding molecular ion peak of  $2$  was observed at  $m/z = 1833.0512$ , indicative of the formation of a mononuclear zinc complex. The 400 Mz  $^1H$  NMR spectrum of  $2$  in  $CDCl_3$  exhibits only two NH peaks at  $\delta = 12.50$  and 7.54 ppm (Figures S4 and S14), indicating that a zinc(II) cation was accommodated in the pyrrolic environment of  $1$ .

The X-ray structure for complex  $2$  supports the atom connectivity of the ligand as established by synthesis and NMR assignment, and establishes explicitly the site for  $Zn^{2+}$  coordination (Figure 3a).<sup>13</sup> The  $Zn^{II}$  coordinated structure of

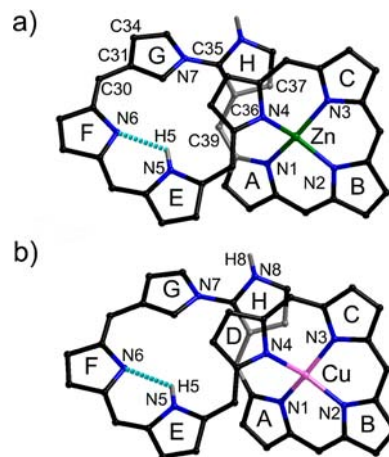


**Figure 3.** Crystal structures of the complex (a)  $2$  and (b)  $3$ . *meso*- $C_6F_5$  groups and the hydrogens atoms are omitted for clarity.

$1$  revealed a figure-of-eight conformation. One zinc atom resides within the  $N_4$  cavity donated by four regularly linked pyrrolic units (A–D), with other four pyrroles (E–H) left noncoordinated. It should be noted that a  $C_\alpha$ –N linkage is present between the two terminal confused pyrroles in the octapyrrenin framework (Figure S15).<sup>10,14</sup> The bond lengths for C30–C31, C31–C34, C36–C37, C36–C39, and C35–N7 lie in the range of 1.414(1)–1.463(1) Å, typical of C–C and C–N single bonds, which can be used for the assignment of the carbon and the nitrogen atoms.<sup>9,10</sup> Within the macrocycle, N6 is hydrogen bonded to H5 with the  $N5 \cdots N6$  distance of 2.82 Å. Similar to the corresponding neo-confused hexapyrrenin,<sup>10a</sup> the

octaphyrin **2** is highly distorted. The A/B, B/C, and C/D interplanar angles within the coordinated tetrapyrin unit are observed to be 29.3°, 10.5°, and 13.8°, respectively. The noncoordinated tetrapyrrolic unit is more severely distorted, with E/F, F/G, and G/H interplanar angles of 46.0°, 13.3°, and 12.1°, respectively. As inferred from the comparative NMR analysis (e.g., the presence of one outward NH and three inner NH moieties), the structure of freebase **1** could also adopt the figure-of-eight structure as seen in complex **2**.

Likewise, the reaction of **1** with Cu(OAc)<sub>2</sub>·H<sub>2</sub>O under identical conditions yielded the corresponding mononuclear copper(II) complex **3** in a 87% yield. Complex **3** is paramagnetic due to the presence of a d<sup>9</sup> electronic Cu<sup>II</sup> center. Thus, the electron paramagnetic resonance (EPR) spectrum of **3** was determined in CH<sub>2</sub>Cl<sub>2</sub> at 100 K (Figure S16). Characteristic *g* tensors (e.g., *g*<sub>⊥</sub> = 2.04, *g*<sub>∥</sub> = 2.23) were observed with four hyperfine splittings derived from the coupling of a copper nucleus and the unpaired electron. On this basis, the geometric configuration of the Cu<sup>II</sup> center in **3** is likely square-planar.

Accordingly, the crystal structure of the copper complex **3** was also elucidated to resemble to that of zinc complex **2** (Figure 3b).<sup>13</sup> The Cu<sup>II</sup> cation is stationed at the N4 cavity of the octaphyrin. The C<sub>α</sub>-N linkage between two terminal confused pyrroles is estimated to be 1.411(1) Å. Due to the similarity between the ionic radii of two metal cations, the whole geometry of the complex **3** is thus not dramatically influenced by the metal ions.

Consistent with the distinct nonaromatic nature of the octaphyrins, UV-vis absorption spectra of **1–3** exhibit broad featureless bands with comparable intensities in the whole visible-near-infrared region (Figure 4). The freebase **1** shows

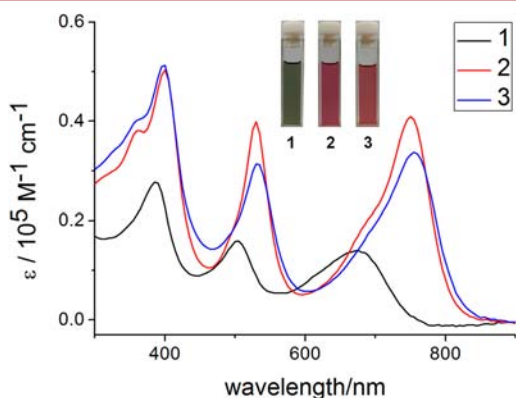


**Figure 4.** Absorption spectra of **1–3** in CH<sub>2</sub>Cl<sub>2</sub>. The inset shows the photographs of these compounds in CH<sub>2</sub>Cl<sub>2</sub>.

three distinct absorption maxima at 385, 505, and 675 nm, while upon complexation of metal cations, the corresponding bands are red-shifted, with the lowest energy peaks at 750 and 755 nm for **2** and **3**, respectively.

In an effort to identify the HOMO–LUMO energy gaps of the compounds **1–3**, the electrochemical properties were analyzed by cyclic voltammetry in CH<sub>2</sub>Cl<sub>2</sub> containing 0.1 M tetra-*n*-butylammonium perchlorate (TBAP) under an inert atmosphere (Table 1 and Figure S17). Three oxidations were observed for compound **1**, and the first two were reversible. Four reductions were observed, the last of which was irreversible at a scan rate of 0.10 V/s. Compounds **2** and **3** display similar electrochemical features, showing three

**Table 1.** Electrochemical Data for Compounds **1–3**

	oxidation (V)		reduction (V)			$\Delta E$ (eV) <sup>a</sup>
	$E^{1/2}_{ox2}$	$E^{1/2}_{ox1}$	$E^{1/2}_{red1}$	$E^{1/2}_{red2}$	$E^{1/2}_{red3}$	
<b>1</b>	0.84	0.72	−0.37	−0.70	−1.07	1.09
<b>2</b>	0.94	0.51	−0.47	−0.80	−	0.98
<b>3</b>	0.95	0.53	−0.47	−0.79	−	1.00

<sup>a</sup> $\Delta E = E^{1/2}_{ox1} - E^{1/2}_{red1}$ .

oxidations and three major reductions in CH<sub>2</sub>Cl<sub>2</sub> as seen in Figure S17. The electrochemically measured HOMO–LUMO gap is 1.09 eV for **1**, 0.98 eV for **2**, and 1.00 eV for **3** under the given experimental conditions.

To gain further insight into the electronic properties of the octaphyrins, density functional theory (DFT) calculations were carried out for compounds **1–3** using the Gaussian 09 program package.<sup>15</sup> The optimized structures were obtained based on the X-ray crystal structures and the HOMO–LUMO gaps of **1–3** were calculated to be 1.48, 1.37, and 1.38 eV, respectively (Figures S18–S20 and Table S1). The trend is in good agreement with that observed from the electrochemical data. The coordination of zinc and copper cations led to a slight destabilization of the highest occupied molecular orbitals (HOMOs), resulting in narrower HOMO–LUMO gaps relative to the free base **1**. This alteration of the MOs is corresponding to the time-dependent (TD) DFT calculations, which support the experimental absorption bands (Figure S21). Furthermore, the nucleus-independent chemical shift (NICS) calculations at the global centers of the macrocycles for **1** and **2** gave nearly zero values (i.e., 0.6 and 1.3 ppm, respectively), which is indicative of nonaromaticity for the macrocycles (Tables S2 and S3). In addition, the visualization of induced electronic delocalization was attempted, to obtain the information on the electron delocalization. Anisotropy of the induced current density (AICD) plots<sup>16</sup> revealed less conjugated delocalization on the circuit with random density vectors for compounds **1** and **2**. Intriguingly, the particular density of an N-linking bond between the confused rings was found, which implies the effective conjugation over the C<sub>α</sub>-N bonding fashion present in the macrocycles (Figure S22).

In summary, we have successfully synthesized and characterized novel *meso*-C<sub>6</sub>F<sub>5</sub> substituted octaphyrin(1.1.1.1.1.1.0) **1** possessing an interesting N-linkage between two confused rings. The macrocycle **1** exhibits unique coordination abilities, selectively affording mononuclear Zn<sup>II</sup> and Cu<sup>II</sup> complexes, **2** and **3**, respectively. These complexes adopt figure-of-eight conformations and show intrinsic nonaromatic character on the 34 $\pi$  electron conjugation circuit. In conclusion, the ring closure reaction of the octaphyrane with two terminal  $\beta$ -linked pyrroles enables the production of unprecedented neo-confused octaphyrin embedded with a unique N–C<sub>α</sub> bond, which exhibits unique coordination behavior and nonaromaticity.

## ■ ASSOCIATED CONTENT

### Supporting Information

The Supporting Information is available free of charge on the ACS Publications website at DOI: 10.1021/acs.orglett.5b02363.

Complete experimental details; spectroscopic and analytical data, details on DFT calculations (PDF)

Crystallographic data for **2** (CIF)

Crystallographic data for **3** (CIF)

## ■ AUTHOR INFORMATION

## Corresponding Authors

\*E-mail: hfuruta@cstf.kyushu-u.ac.jp

\*E-mail: yshxie@ecust.edu.cn

## Notes

The authors declare no competing financial interest.

## ■ ACKNOWLEDGMENTS

This work was supported by NSFC/China (21472047, 91227201), and the Oriental Scholarship. Support is acknowledged by the Grant-in-Aid (25248039 to H.F. and 26810024 to M.I.) from the JSPS.

## ■ REFERENCES

- (1) (a) Stepien, M.; Sprutta, N.; Latos-Grażyński, L. *Angew. Chem., Int. Ed.* **2011**, *50*, 4288. (b) Roznyatovskiy, V. V.; Lee, C. H.; Sessler, J. L. *Chem. Soc. Rev.* **2013**, *42*, 1921. (c) Xie, Y. S.; Yamaguchi, K.; Toganoh, M.; Uno, H.; Suzuki, M.; Mori, S.; Saito, S.; Osuka, A.; Furuta, H. *Angew. Chem., Int. Ed.* **2009**, *48*, 5496. (d) Ding, Y. B.; Tang, Y. Y.; Zhu, W. H.; Xie, Y. S. *Chem. Soc. Rev.* **2015**, *44*, 1101. (e) Wang, Y. Q.; Chen, B.; Wu, W. J.; Li, X.; Zhu, W. H.; Tian, H.; Xie, Y. S. *Angew. Chem., Int. Ed.* **2014**, *53*, 10779. (f) Sun, X.; Wang, Y. Q.; Li, X.; Ågren, H.; Zhu, W. H.; Tian, H.; Xie, Y. S. *Chem. Commun.* **2014**, *50*, 15609. (g) Li, Z.; Li, Q. Q. *Sci. China: Chem.* **2014**, *57*, 1491. (h) Wei, T. T.; Sun, X.; Li, X.; Ågren, H.; Xie, Y. S. *ACS Appl. Mater. Interfaces* **2015**, DOI: 10.1021/acsami.5b06610. (i) Li, R. S.; Lammer, A. D.; Ferrence, G. M.; Lash, T. D. *J. Org. Chem.* **2014**, *79*, 4078. (j) Lash, T. D.; Lammer, A. D.; Ferrence, G. M. *Angew. Chem., Int. Ed.* **2011**, *50*, 9718.
- (2) (a) Aviv, I.; Gross, Z. *Chem. Commun.* **2007**, *20*, 1987. (b) Flamigni, L.; Gryko, D. T. *Chem. Soc. Rev.* **2009**, *38*, 1635. (c) Aviv-Harel, I.; Gross, Z. *Coord. Chem. Rev.* **2011**, *255*, 717.
- (3) (a) Sessler, J. L.; Seidel, D. *Angew. Chem., Int. Ed.* **2003**, *42*, 5134. (b) Misra, R.; Chandrashekar, T. K. *Acc. Chem. Res.* **2008**, *41*, 265.
- (4) Furuta, H.; Ogawa, T.; Asano, T. *J. Am. Chem. Soc.* **1994**, *116*, 767.
- (5) Chmielewski, P. J.; Latos-Grażyński, L.; Rachlewicz, K.; Głowiak, T. *Angew. Chem., Int. Ed. Engl.* **1994**, *33*, 779.
- (6) (a) Toganoh, M.; Furuta, H. *Chem. Commun.* **2012**, *48*, 937. (b) Srinivasan, A.; Furuta, H. *Acc. Chem. Res.* **2005**, *38*, 10.
- (7) (a) Toganoh, M.; Sato, A.; Furuta, H. *Angew. Chem., Int. Ed.* **2011**, *50*, 2752. (b) Fujino, K.; Hirata, Y.; Kawabe, Y.; Morimoto, T.; Srinivasan, A.; Toganoh, M.; Miseki, Y.; Kudo, A.; Furuta, H. *Angew. Chem., Int. Ed.* **2011**, *50*, 6855.
- (8) (a) Gadekar, S. C.; Reddy, B. K.; Anand, V. G. *Angew. Chem., Int. Ed.* **2013**, *52*, 7164. (b) Gokulnath, S.; Yamaguchi, K.; Toganoh, M.; Mori, S.; Uno, H.; Furuta, H. *Angew. Chem.* **2011**, *123*, 2350. (c) Gokulnath, S.; Nishimura, K.; Toganoh, M.; Mori, S.; Furuta, H. *Angew. Chem., Int. Ed.* **2013**, *52*, 6940.
- (9) Xie, Y. S.; Wei, P. C.; Li, X.; Hong, T.; Zhang, K.; Furuta, H. *J. Am. Chem. Soc.* **2013**, *135*, 19119.
- (10) (a) Wei, P. C.; Zhang, K.; Li, X.; Meng, D. Y.; Ågren, H.; Ou, Z. P.; Ng, S.; Furuta, H.; Xie, Y. S. *Angew. Chem., Int. Ed.* **2014**, *53*, 14069. (b) D'Souza, F. *Angew. Chem., Int. Ed.* **2015**, *54*, 4713.
- (11) Zhang, K.; Wei, P. C.; Li, X.; Ågren, H.; Xie, Y. S. *Org. Lett.* **2014**, *16*, 6354.
- (12) (a) Shimizu, S.; Tanaka, Y.; Youfu, K.; Osuka, A. *Angew. Chem., Int. Ed.* **2005**, *44*, 3726. (b) Tanaka, Y.; Mori, H.; Koide, T.; Yorimitsu, H.; Aratani, N.; Osuka, A. *Angew. Chem., Int. Ed.* **2011**, *50*, 11460. (c) Latos-Grażyński, L. *Angew. Chem., Int. Ed.* **2004**, *43*, 5124.
- (13) CCDC 1418590 (2) and 1418591 (3) contain the supplementary crystallographic data for this paper. These data can be obtained free of charge from The Cambridge Crystallographic Data Centre via [www.ccdc.cam.ac.uk/data\\_request/cif](http://www.ccdc.cam.ac.uk/data_request/cif).
- (14) Hisamune, Y.; Nishimura, K.; Isakari, K.; Ishida, M.; Mori, S.; Karasawa, S.; Kato, T.; Lee, S.; Kim, D.; Furuta, H. *Angew. Chem., Int. Ed.* **2015**, *54*, 7323.
- (15) All the calculations were achieved with Gaussian09 program package at the B3LYP/6-31G\* level. See Supporting Information for calculation details.
- (16) Geuenich, D.; Hess, K.; Köhler, F.; Herges, R. *Chem. Rev.* **2005**, *105*, 3758.